

Vascular Biology, Atherosclerosis and Endothelium Biology

Lymphatic Precollectors Contain a Novel, Specialized Subpopulation of Podoplanin^{low}, CCL27-Expressing Lymphatic Endothelial Cells

Nikolaus Wick,* Daniela Haluza,*
Elisabeth Gurnhofer,* Ingrid Raab,*
Marie-Theres Kasimir,† Michael Prinz,‡
Carl-Walter Steiner,§ Christina Reinisch,¶
Anny Howorka,* Pietro Giovanoli,||**
Sabine Buchsbaum,|| Sigurd Krieger,*
Erwin Tschachler,¶ Peter Petzelbauer,††
and Dentscho Kerjaschki*

From the Department of Pathology, the Department of Surgery,†
Division of Cardiac-Thoracic Surgery; the Core Unit for Medical
Statistics and Informatics;‡ the Department of Internal Medicine,§
Division of Rheumatology; the Department of Dermatology,¶
Research Unit of Biology and Pathobiology of Human Skin; the
Department of Surgery,|| Division of Plastic and Reconstructive
Surgery; and the Department of Dermatology,†† Division of
General Dermatology, Vienna Medical University, Vienna,
Austria; and the Department of Reconstructive Surgery,**
University Hospital Zurich, Zurich, Switzerland*

Expression of the lymphoendothelial marker membrane mucoprotein podoplanin (podo) distinguishes endothelial cells of both blood and lymphatic lineages. We have previously discovered two distinct subpopulations of lymphatic endothelial cells (LECs) in human skin that were defined by their cell surface densities of podoplanin and were designated LEC^{podo-low} and LEC^{podo-high}. LEC^{podo-low} is restricted to lymphatic precollector vessels that originate from initial LEC^{podo-high}-containing lymphatic capillaries and selectively express several pro-inflammatory factors. In addition to the chemokine receptor protein Duffy blood group antigen receptor for chemokines, these factors include the constitutively expressed chemokine CCL27, which is responsible for the accumulation of pathogenic CCR10⁺ T lymphocytes in human inflammatory skin diseases. In this study, we report that CCR10⁺ T cells accumulate preferentially both around and within CCL27⁺ LEC^{podo-low} precollector vessels in skin biopsies of human inflammatory disease. In transmigration assays, isolated CCR10⁺ T lymphocytes are chemotactically attracted by LEC^{podo-low} in a CCL27-dependent fashion, but not by LEC^{podo-high}. These observations indicate that

LEC^{podo-low}-containing precollector vessels constitute a specialized segment of the initial lymphatic microvasculature, and we hypothesize that these LEC^{podo-low}-containing vessels are involved in the trafficking of CCR10⁺ T cells during skin inflammation. (*Am J Pathol* 2008, 173:1202–1209; DOI: 10.2353/ajpath.2008.080101)

The dermal lymphatic microvasculature drains interstitial fluid and passenger cells into lymph nodes. Its complex microanatomy was previously cartographed by tracer injections and found to consist of superficial initial, blind-ending capillaries that are linked via precollectors to deep collecting vessels.¹ It is commonly believed that initial capillaries constitute the principal site of lymphatic function and that they provide exit routes for cells from the interstitial compartment, eg, antigen-presenting cells, in normal tissues and “spent” pathogenic lymphocytes in inflammation. By contrast, the subsequent precollectors and collectors are considered as passive sewer systems. However, there is no definite experimental proof for this naïve concept. A possible clue to potentially different functions of these vascular segments could be provided by distinct properties of endothelial cells in each compartment, but also, no information exists about lymphatic endothelial cell (LEC) heterogeneity. Here, we report the existence of two distinct subpopulations of LECs that are distinguished by their differential expression of the general LEC marker podoplanin and other molecules, such as pro-inflammatory chemokines. We demonstrate that these LEC subpopulations strictly associate with initial lymphatic capillaries and precollectors, respectively, and we examine their potential functional diversity in inflammatory skin diseases.

Supported by the Austrian Science Foundation (16472-B08), the Vienna Science and Technology Fund (LS139), the EU-FP6 framework program Lymphangio-genomics (LSHG-CT-2004-503573), and the Austrian Ministry for Education (Trafo Program).

Accepted for publication June 24, 2008.

Address reprint requests to Dentscho Kerjaschki, Department of Pathology, Vienna Medical University, Waehringer Guertel 18–20, A-1090 Vienna, Austria. E-mail: dentscho.kerjaschki@meduniwien.ac.at.

Materials and Methods

Isolation of Endothelial Cells

Blood vascular endothelial cells (BECs) and LECs were isolated *ex vivo* from dermatome skin sheets from cosmetic breast surgery specimens of healthy females, in a two step protocol using mechanical and enzymatic dissociation, followed by fluorescence-activated cell sorting (FACStar Plus; BD Biosciences, Franklin Lakes, NJ) using CD45 antibodies for gating and CD31 and podoplanin antibodies for separation as reported previously.^{2,3} LEC^{pod_o-low} and LEC^{pod_o-high} were purified by fluorescence-activated cell sorting separation of the total LEC fraction by increasing the resolution of the podoplanin channel. The collected cells were lysed for RNA isolation or immobilized on slides by cytospin (Cytospin 3; Dako Cytomation, Glostrup, Denmark) or taken into tissue culture. The study complied with the Declaration of Helsinki and was as approved by the local ethics committee (permit no. 449/2001).

Antibodies

We used the IgG fraction of a rabbit polyclonal anti-podoplanin and of the corresponding preimmune serum.^{3,4} The other reagents were FITC-conjugated monoclonal anti-CD31 (catalog no. 555445; BD Biosciences Pharmingen, Franklin Lakes, NJ), RPE-Cy5.1-conjugated mouse monoclonal anti-CD45 (catalog no. PM IM2653; Beckman Coulter, Inc., Fullerton, CA), mouse clone 2C3 anti-Duffy blood group antigen receptor for chemokines (DARC)/Fy (kindly provided by Dr. Yves Colin; INSERM, Institut National de Transfusion Sanguine, Paris^{5,6}), mouse monoclonal anti-CCL27 (catalog no. MAB3761; R&D Systems, Minneapolis, MN), neutralizing rat anti-CCL27 antibody (clone 68623; catalog no. MAB725; R&D Systems), rat IgG-Isotype control (catalog no. ab37361; Abcam, Cambridge, UK), mouse monoclonal anti-CCL21 (catalog no. AF366; R&D Systems), goat polyclonal anti-CCR10 (catalog no. NB 100-707; Novus Biologicals, Littleton, CO), rat monoclonal anti-human CLA antibody (catalog no. 55946; BD Biosciences Pharmingen), mouse monoclonal anti-CD31 (catalog no. M0823; Dako Cytomation), and phycoerythrin-conjugated mouse monoclonal anti-CD3 (catalog no. 345765; Becton Dickinson) antibodies. Secondary agents were phycoerythrin-conjugated donkey polyclonal anti-rabbit IgG (WG, catalog no. 711-116-152; Jackson ImmunoResearch Laboratories, Inc., West Grove, PA), Alexa Fluor 594-conjugated goat anti-mouse and Alexa Fluor 488- and 350-conjugated goat anti-rabbit (1 μ g/ml; nos. catalog nos. A-11020, A-11034 and A-11046; Molecular Probes, Inc., Eugene, OR), and 10 nm gold-labeled goat anti-rabbit (catalog no. RPN421; Amersham Biosciences, Uppsala, Sweden) antibodies.

RNA Analysis

Isolation of total RNA, generation of cRNA, and DNA chip hybridization were performed as described previously.⁴

DNA chip hybridization was performed on GeneChip U133A (Affymetrix, Inc., Santa Clara, CA). Raw and processed data were deposited at ArrayExpress (accession no. E-TABM-227). DNA chip raw data were normalized to a subset of 10 housekeeping genes using MAS 5.0 software and exported as spreadsheets. Considering the sample size of $n = 2$, only postnormalized probe set values tagged as "present" were accepted. Ratios of values of LEC^{pod_o-low} and LEC^{pod_o-high} sample pairs deriving from each patient were calculated. Both ratios were averaged, and a threshold of differential induction of \geq fivefold was applied. Finally, bibliographic search on PubMed database for co-occurrence of the gene name and the keywords "skin" and "chemokine" defined a selected list of eight genes induced in LEC^{pod_o-low} versus LEC^{pod_o-high}. The two housekeeping genes in nonquantitative RT-PCR were breakpoint cluster region and β 2-microglobulin, as described previously.³ In addition, early passage cultures of LEC^{pod_o-low} and LEC^{pod_o-high} were subjected to quantitative real-time PCR (Applied Biosystems, Foster City, CA) for relative podoplanin mRNA quantification using $\Delta\Delta$ Ct.

Morphological Analysis

For electron microscopy, human skin was fixed in 4% PFA and 0.1% glutaraldehyde and embedded in Lowicryl-K4M, and sections were immunolabeled with 20 μ g/ml anti-podoplanin antibody, followed by 10 nm goat anti-rabbit gold conjugate (final concentration, 1:10). The number of gold particles bound to \sim 500 μ m of LEC plasma membranes were counted and expressed as number of gold particles per 1 μ m. Lymphatic capillaries were identified by their expression of podoplanin, the absence of continuous basement membranes, and lack of erythrocytes in their lumen.

For reconstruction of lymphatic vessels in three dimensions, double immunofluorescence was performed on 100 μ m cryostat sections of tissue samples that were fixed in 4% PFA for 1.5 hours at 22°C, immersed into 30% sucrose at 4°C overnight, and frozen in liquid nitrogen.⁷ The sections were immunolabeled with antibodies against podoplanin (2.8 μ g/ml) and CCL27 (2.5 μ g/ml). After extensive washing, they were postfixed in 4% paraformaldehyde for 10 minutes at 22°C and permeabilized with 0.3% Triton X-100 for 60 minutes. Primary antibodies were incubated for 3 days at 22°C, and secondary antibodies were incubated for 6 hours. Sections were analyzed by confocal laser scanning microscopy using a Zeiss LSM 510 (Carl Zeiss, Jena, Germany). Three-dimensional visualization was realized in a program in JAVA, based on the Visualization Toolkit 5.0 (Kitware, Clifton Park, NY; <http://www.vtk.org>). Negative controls omitting the first antibodies consistently gave negative results, as did incubation with nonimmune sera (data not shown).

Immunofluorescence labeling was performed on 2- μ m paraffin sections of formaldehyde-fixed human tissues. After antigen retrieval by microwaving twice for 5 minutes in 0.01 mol/L citrate buffer, pH 6, primary antibodies were combined with antibodies conjugated to fluorescent dyes

for double or triple staining.⁸ Images were captured with the Axiophot epifluorescence system (Zeiss). We combined immunolabeling by antibodies toward podoplanin with those specific for DARC (final concentration 20 $\mu\text{g}/\text{ml}$), CCL21 (15 $\mu\text{g}/\text{ml}$), CCR10 (4 $\mu\text{g}/\text{ml}$), and CCL27. For quantification of the distribution of CCR10⁺ in the perivascular stroma, the perilymphatic area was divided into concentric rings of incremental 10- μm radiuses (R1–3) measured from the vessel's outer surface, and CCR10⁺ cells were counted in each segment and normalized to 1000 μm^2 . Also, the number of CCR10⁺ cells was determined in the vascular lumen.

Cell Culture

Culturing of human LEC subpopulations was performed on 10 $\mu\text{g}/\text{ml}$ fibronectin-coated dishes (catalog no. 354008; BD Biosciences) in EGM-2MV complete growth medium (catalog no. CC-3202; Cambrex, Inc., East Rutherford, NJ). Cells were detached by 1 \times trypsin-EDTA (catalog no. 25300-05; Invitrogen, Carlsbad, CA), lysed in SDS sample buffer, and analyzed by reduced gel electrophoresis and Western blotting. For immunofluorescence, endothelial cells were fixed for 15 minutes at 22°C in 4% paraformaldehyde. Nuclei were stained with 10 $\mu\text{g}/\text{ml}$ 4',6'-diamidino-2-phenylindole hydrochloride (SERVA GmbH, Heidelberg, Germany). The concentration of CCL27 in tissue culture supernatants was determined by ELISA (R&D Systems).

Transmigration Assays

BECs, LEC^{pod_o-low}, and LEC^{pod_o-high} were seeded onto the bottom of transwell dishes with polycarbonate membrane inserts with 5- μm pores (catalog no. 3421; Costar, Cambridge, MA).⁹ CD3⁺ CCR10⁺ human peripheral blood T lymphocytes were purified from pooled human blood samples by fluorescence-activated cell sorting, labeled with CellTracker (2 $\mu\text{g}/\text{ml}$ CellTracker green CMFDA; catalog no. C2925; Invitrogen), and resuspended in 100 μl RPMI with 10% fetal calf serum; and 1 \times 10⁵ cells were added into the top chamber of each insert. After 4 hours, the *trans*-migrated cells in the lower chamber were collected by cytospinning onto microscope slides and counted in a fluorescence microscope. Fixed cells were additionally immunostained with 10 $\mu\text{g}/\text{ml}$ anti-CLA antibody. In some experiments, 10 $\mu\text{g}/\text{ml}$ neutralizing monoclonal rat anti-CCL27 antibody was added into the bottom chamber. As control, isotype matched irrelevant rat IgG was used in the same concentration in parallel experiments.

Statistical Analysis

All quantitative experiments were performed at least in triplicate (RT-PCR, numbers of immunogold particles per micrometer of LEC cell membrane representing podoplanin, capillary densities in histological sections, localization of CCR10⁺ T lymphocytes in relation to lymphatic vessels *in situ*, and CCR10⁺ T-lymphocyte transmigration assays), and the results were subjected to the two-sided Student's *t*-test.

Results

Differential Expression of Podoplanin in Two Distinct LEC Subpopulations

The fluorescence-activated cell sorting pattern of isolated dermal microvascular CD45⁻CD31⁺Podoplanin⁺ LECs and CD45⁻CD31⁺Podoplanin⁻ BECs has previously suggested the presence of two overlapping LEC subpopulations that varied in their surface expression of podoplanin.² Here, we have isolated these two LEC cohorts, and designated them as LEC^{pod_o-low} and LEC^{pod_o-high} (Figure 1A). The distinctly different levels of podoplanin expression of LEC^{pod_o-low} and LEC^{pod_o-high} were confirmed by indirect immunofluorescence in *ex vivo* cytospin preparations (Figure 1B), and their lymphatic phenotype was supported by nonquantitative RT-PCR for the established LEC markers LYVE-1, Prox1, and the pan-endothelial marker von Willebrand factor (Figure 1, C and F). In cell culture, small amounts of podoplanin protein were detected by Western blotting in LEC^{pod_o-low} that, however, remained abundant in LEC^{pod_o-high} (Figure 1D). This was also confirmed at the level of mRNA by quantitative RT-PCR (Figure 1E). In later passages, the expression of podoplanin in LEC^{pod_o-low} increased toward the levels of LEC^{pod_o-high}, whereas the expression of the LEC^{pod_o-low} typical chemokine CCL27 (Figure 1G) was lost after the second passage (data not shown).

Restricted Localization of LEC^{pod_o-low} in Lymphatic Precollectors

To identify additional markers for the precise localization of LEC^{pod_o-low} and to gain insight into the LEC^{pod_o-low}'s distinct phenotype in normal and particularly in inflamed tissues, a DNA chip analysis was performed in a shotgun approach. We purified RNA from freshly isolated LEC^{pod_o-low}, LEC^{pod_o-high}, total LECs, and total BECs^{2,3} that were isolated from the dermis of two patients without skin disease. In Affymetrix arrays, we identified 107 genes that were amplified by at least fivefold in LEC^{pod_o-low}. Of these, eight were associated with inflammation (Table 1) and included members of the chemokine/chemokine receptor family, such as *Ccl27*, *Cxcl12*, *Cxcl14*, and *Darc*. In addition, LEC^{pod_o-low} overexpressed E-selectin, components of the major histocompatibility complex type II (MHC II), and placental growth factor. By contrast, LEC^{pod_o-high} significantly overexpressed *Ccl21*. The chemokine CCL27 was expressed in cultured LEC^{pod_o-low}, but not in LEC^{pod_o-high} (Figure 1G), and released into cell culture media in a concentration <1 ng/ml.

For immunohistochemical colocalization of LEC^{pod_o-low} with podoplanin, we selected CCL27 (CTACK),¹⁰ an established pathogenic chemokine in dermal inflammatory diseases that was robustly expressed by LEC^{pod_o-low}, but not by LEC^{pod_o-high}, and the chemokine binding protein DARC,¹¹ taking advantage of its nondiffusibility as a membrane protein. The results of these colocalization studies indicated that LEC^{pod_o-low} were restricted exclusively to a distinct segment of the lymphatic vasculature,

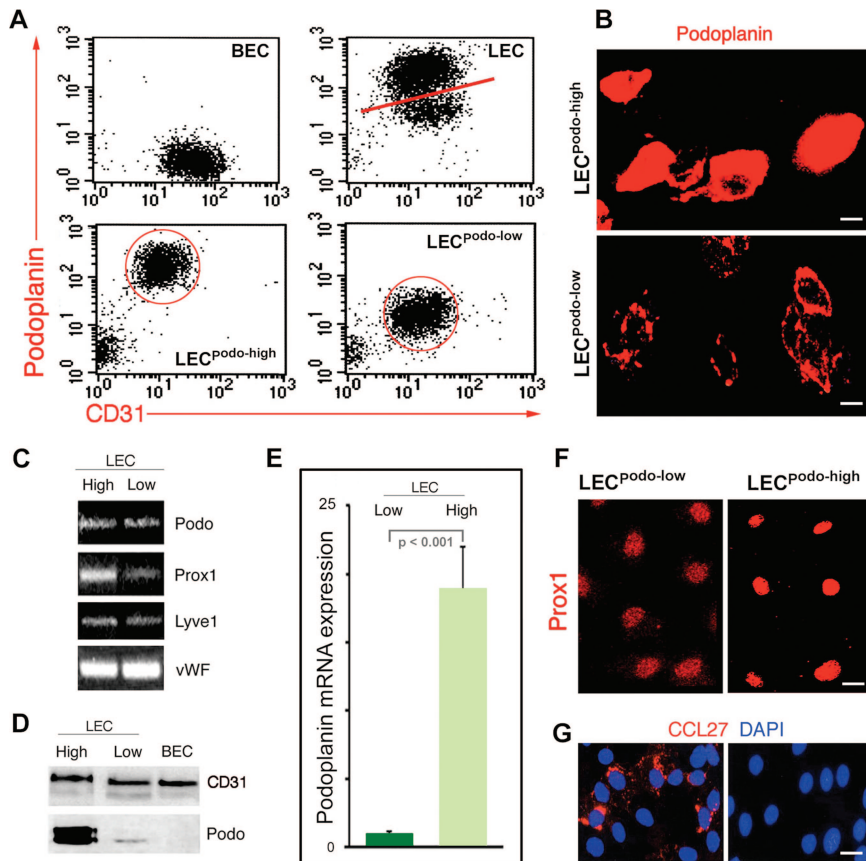


Figure 1. *Ex vivo* isolation, *in vitro* expansion, and characterization of LEC^{podo-low} and LEC^{podo-high}. **A:** BECs, LECs, LEC^{podo-low}, and LEC^{podo-high} were separated by fluorescence-activated cell sorting *ex vivo* from CD45-gated human dermatome skin cell suspensions, using CD31 and podoplanin antibodies. CD31⁺ podoplanin⁻ BECs (*top left*), CD31⁺ podoplanin⁺ total LECs (*top right*, the red bar separates two overlapping subpopulations), CD31⁺ podoplanin^{high} LECs (*bottom left*, red circle), and CD31⁺ podoplanin^{low} LECs (*bottom right*, red circle) are resolved. **B:** Cytospin preparations of *ex vivo* isolated LEC^{podo-low} and LEC^{podo-high} show differential podoplanin expression by immunofluorescence. **C:** Nonquantitative RT-PCR reveals the expression of the LEC marker genes Prox1 and LYVE-1, and the pan-endothelial marker von Willebrand factor (*vWF*) in LEC^{podo-low} and LEC^{podo-high}. **D:** After two rounds of expansion in tissue culture of LEC^{podo-low} and LEC^{podo-high}, the differential expression of podoplanin protein is confirmed by immunoblotting and related to CD31 expression. **E:** Quantitative RT-PCR confirmed the different levels of podoplanin mRNA expression ($P < 0.001$). **F:** Prox1 is stably expressed in cultured LEC^{podo-low} and more abundant in LEC^{podo-high}, whereas expression of the LEC^{podo-low} specific marker CCL27, indicated here by red immunofluorescence in cultured LEC^{podo-low} (**G, left**) is lost after the third passage in cell culture. LEC^{podo-high} fail to express CCL27 (**G, right**). All bars = 10 μ m.

separate from LEC^{podo-high} vessels (Figure 2A). Within single lymphatic vessels, there was consistently no intermixing of the two LEC subpopulations. Immunoelectron microscopy also confirmed the at least fourfold different podoplanin content on the plasma membrane surface of LEC^{podo-low} and LEC^{podo-high} (Figure 2B).

To determine the topographic relation of LEC^{podo-low} and LEC^{podo-high} in the lymphatic vasculature, we reconstructed in three dimensions consecutive confocal images of 100- μ m-thick sections of normal human skin that

were double labeled for podoplanin and CCL27 or DARC. The images obtained demonstrated that LEC^{podo-low} were restricted to precollector vessels that branch out of LEC^{podo-high} initial lymphatic capillaries (Figure 2C). The latter exclusively expressed CCL21¹² and large amounts of podoplanin, in contrast to LEC^{podo-low} vessels that were immunolabeled for CCL27 (Figure 2D). This indicated that LEC^{podo-low} were restricted to lymphatic precollectors that directly originate from canonical initial LEC^{podo-high} lymphatic capillaries, and that the LEC sub-

Table 1. Inflammation-Associated Genes in LEC^{podo-low}

Genes	Podo-low	Podo-high	Total LEC	Total BEC	Podo-low/high
Markers used in this study					
<i>Ccl27</i> (chemokine CC motif ligand 27, cutaneous T cell-attracting chemokine/ <i>Ctack</i>)	1293.3	176.4	343.6	341.7	7.3
<i>Darc</i>	2545.8	480.2	1738.9	3674.5	5.3
<i>Ccl21</i> (chemokine CC motif ligand 21, secondary lymphoid tissue chemokine/ <i>Slc</i>)	66.1	2725.4	2828.6	20.8	0.024
Markers not used in this study					
<i>Cxcl14</i> (chemokine CXC motif ligand 14, breast and kidney/ <i>Brak</i>)	6999.0	902.5	679.2	1105.6	7.8
<i>Cxcl12</i> (chemokine CXC motif ligand 12, stromal cell-derived factor 1/ <i>Sdf1</i>)	1592.3	124.5	100.8	179.8	12.8
E-selectin (endothelial adhesion molecule, <i>Sele</i>)	3201.6	821.6	2828.6	5365.8	3.9
Major histocompatibility complex type II γ (<i>Cd74</i>)	2045.2	471.3	884.0	3561.0	4.3
Major histocompatibility complex type II β DPB1 (<i>Hla-dpb1</i>)	2461.2	384.9	1354.9	4207.0	6.4
<i>Pif</i> (placental growth factor)	8267.6	775.3	507.8	788.3	10.7

Numbers indicate normalized fluorescence signal intensities for LEC^{podo-low}, LEC^{podo-high}, total LEC, and total BEC determined by Affymetrix DNA chip analysis.⁴ Fold ratios between LEC^{podo-low} and LEC^{podo-high} are in the right column.

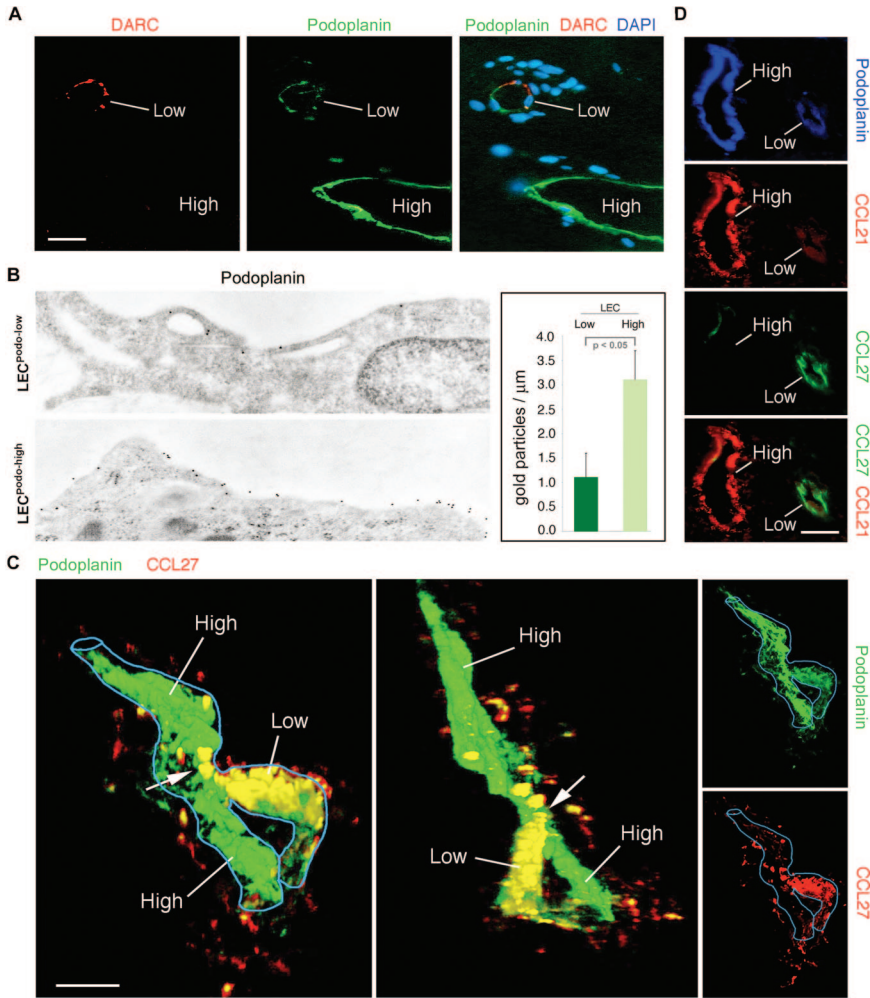


Figure 2. Segmentation of the dermal lymphatic microvasculature into $LEC^{podo-low}$ precollectors and $LEC^{podo-high}$ initial lymphatic capillaries, revealed by expression of distinct marker proteins. **A:** Localization of DARC (left, red), podoplanin (middle, green), and a merged picture with 4',6'-diamidino-2-phenylindole hydrochloride nuclear staining (right, blue). Endothelial cells of the $LEC^{podo-low}$ DARC⁺ type are restricted to a small vessel and do not intermix with the larger $LEC^{podo-high}$ DARC⁻ vessel. **B:** Immunoelectron microscopy supports the differential expression of podoplanin on the luminal cell surfaces of both LEC subpopulations. The density of gold particles that indicate podoplanin differ three- to fourfold ($P < 0.05$). **C:** Three-dimensional reconstruction of the initial lymphatic microvessels in human skin resolved by confocal laser scanning microscopy and subsequent three-dimensional reconstruction of 100- μ m-thick sections, using antibodies specific for podoplanin (green) and CCL27 (red). The $LEC^{podo-low}$ indicators CCL27 and podoplanin^{low} are restricted to a distinct vessel (Low) that branches out of a larger, $LEC^{podo-high}$ CCL27⁻ initial lymphatic capillary (High). Merged versions of rotated presentations of the anastomosing vessels are shown on the left, and single channels on the right. **D:** Triple immunofluorescence showing coexpression of high levels of podoplanin (blue) with CCL21 (red) in $LEC^{podo-high}$ (High) and of lower levels of podoplanin with CCL27 (green) in $LEC^{podo-low}$ (Low). Merge of channels is on the bottom panel. Bars = 10 μ m in A, C, and D. Magnification: $\times 70,000$ (D).

populations expressed the same molecular signatures discovered also *in situ* as seen before in isolated cell. A similar compartmentalization of the lymphatic microvasculature with distinct segregation of $LEC^{podo-high}$ - and $LEC^{podo-low}$ -containing segments was found in 6 samples of normal skin, 15 cases of chronic dermal inflammatory diseases, and in sporadic cases of renal transplant rejection (Figure 3A) and pulmonary disease (Figure 3B).

Increased Dermal Lymphatic Microvascular Density in Inflammatory Skin Diseases

Lymphatic microvessel densities were determined in all samples of normal and inflammatory skin, using podoplanin and CCL27 and/or DARC as immunohistochemical markers. We observed that the overall lymphatic vessel density increased threefold in chronic skin inflammation

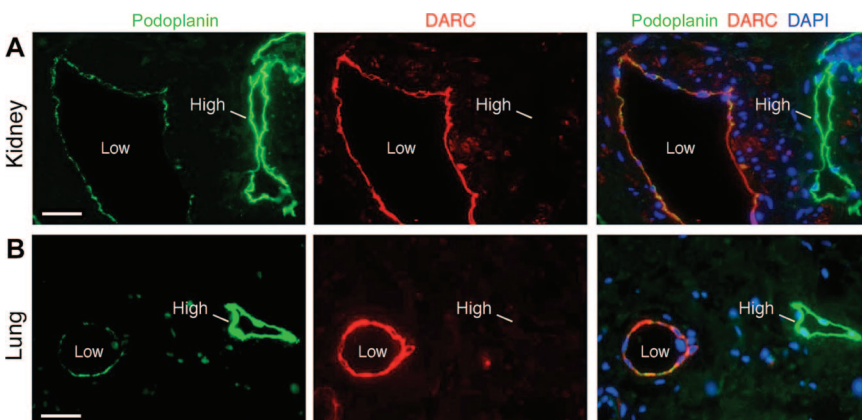


Figure 3. Segregation of $LEC^{podo-low}$ and $LEC^{podo-high}$ vessels in human kidney transplant rejection (A) and chronic bronchiolitis (B). Sections are immunolabeled with antibodies specific for podoplanin (green, left) and DARC (red, middle), and merged (right). DARC expression is restricted to vessels containing $LEC^{podo-low}$ (Low) and absent from those containing $LEC^{podo-high}$ (High). Nuclear 4',6'-diamidino-2-phenylindole hydrochloride stain is blue. Bar = 10 μ m.

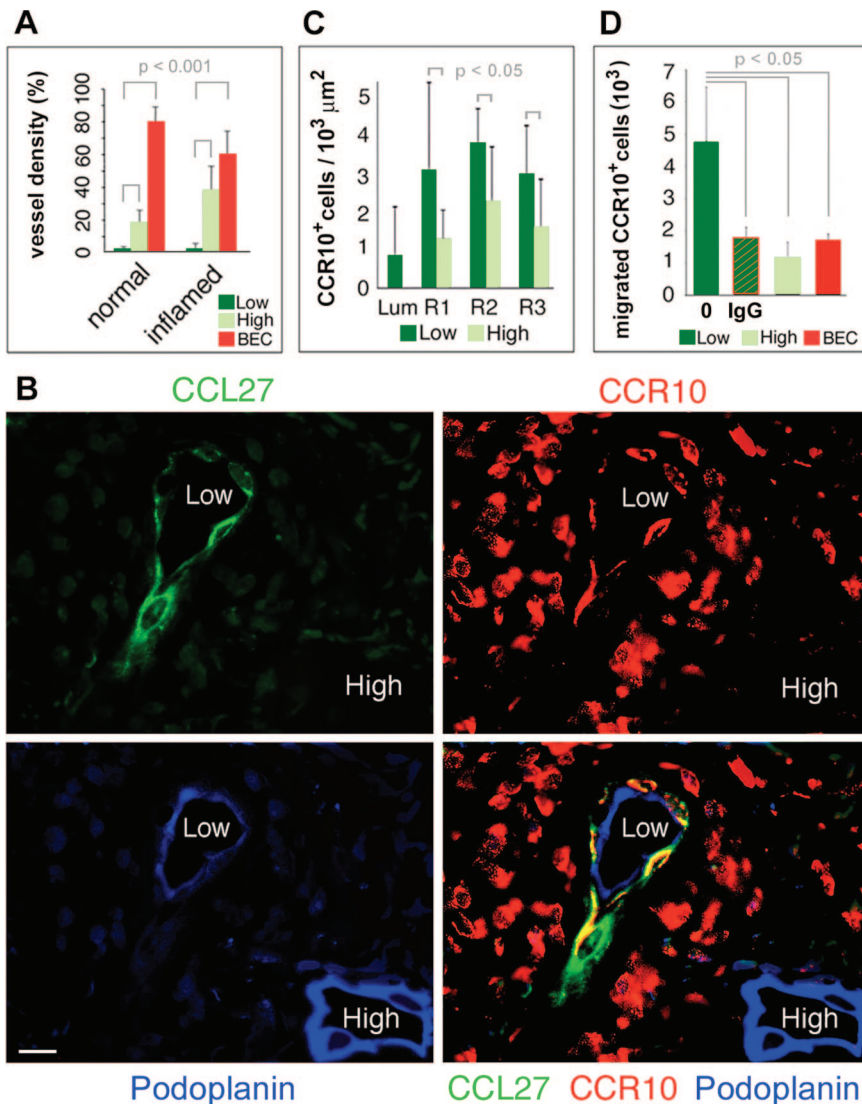


Figure 4. Association of CCR10⁺ T lymphocytes with LEC^{pod-low}-containing lymphatic precollector vessels. **A:** Determination of the blood and lymphatic microvessel densities in normal ($n = 14$) and inflamed human skin samples ($n = 15$) expressed as percentage of the total vessel number counted (all P values < 0.001 ; error bars are SD). The ratio of vessel densities remain constant in normal and inflamed skin. **B:** Sections of a case with atopic dermatitis are immunolabeled for the localization of CCL27 (**top left**, green), podoplanin (**bottom left**, blue), and CCR10 (**top right**, red) and a merged picture on the **bottom right**. CCL27 and podoplanin differentially mark a LEC^{pod-high} initial lymphatic capillary (High) and a LEC^{pod-low} precollector (Low). CCR10 is expressed in inflammatory cells that are centered around the precollector, and it is also expressed in small amounts in LEC^{pod-low} (Low). Bar = 20 μm. **C:** Histogram showing the preferential accumulation of CCR10⁺ T lymphocytes around LEC^{pod-low} precollectors (dark green columns) and LEC^{pod-high} lymphatic capillaries (light green columns) and in the vascular lumen (Lum). R1, R2, and R3 indicate concentric perivascular areas with increasing radius (10 μm) in which the quantitation is performed. T lymphocytes are encountered up to three times more frequently around LEC^{pod-low} precollectors than around LEC^{pod-high} lymphatic capillaries (all P values < 0.05 ; error bars = SD) and are found exclusively within the lumina of LEC^{pod-low} precollectors (Lum). **D:** Chemotactic transmigration assay of isolated human CCR10⁺ CLA⁺ CD3⁺ T lymphocytes toward LEC^{pod-low} (dark green columns), LEC^{pod-high} (light green column), and BECs (red column) grown in the lower compartment of Transwell chambers. Transmigration of T lymphocytes is observed toward LEC^{pod-low} and is reduced by a blocking antibody against CCL27 (Blocking IgG, dark green column, red-shaded) but not by a control IgG (Control, dark green column). Attraction by LEC^{pod-high} and BECs are considered as baseline values (all P values < 0.05 ; error bars = SD).

over normal controls and that the relative proportion between LEC^{pod-high} lymphatic capillaries and LEC^{pod-low} precollectors remained constant. Blood capillaries that were identified by expression of DARC⁺ endothelial cells and erythrocytes were 50 times more abundant than LEC^{pod-low} and seven times more abundant than LEC^{pod-high} microvessels in normal skin and in all disease entities studied (Figure 4A).

Association of LEC^{pod-low} Precollectors with CCR10⁺ T Lymphocytes in Inflammatory Skin Diseases

It is established that in chronic inflammatory skin diseases, the CCL27 receptor CCR10 on CLA⁺ pathogenic T lymphocytes mediates homing to the dermis.¹³ In normal human skin, few sporadic CCR10⁺ T lymphocytes were found in the dermis, without significant relation to microvessels (data not shown). By contrast, CCR10⁺ inflammatory infiltrates in human skin samples of psoriasis ($n = 7$), eczema ($n = 7$), and chronic atrophic acro-

dermatitis ($n = 1$) that constitute almost all lymphocytes in these tissues were centered around CCL27-expressing LEC^{pod-low}, as visualized by triple immunofluorescence (Figure 4B). Quantification of the density of the CCR10⁺ T lymphocytes supported this view, with almost threefold higher densities around LEC^{pod-low}-containing precollectors than LEC^{pod-high} initial capillaries. CCR10⁺ T lymphocytes were found within the precollector's lumen but not in that of initial capillaries (Figure 4C).

Chemotactic Attraction of CCR10⁺ T Cells by LEC^{pod-low} in Vitro

LEC^{pod-low}, but not LEC^{pod-high} expressed (Figure 1G) and secreted small amounts of CCL27 (< 1 ng/ml) into the medium. This raised the possibility to test whether or not CCL27⁺ LEC^{pod-low} could attract CCR10⁺ T lymphocytes also *in vitro*, as suggested by the immunohistological *in vivo* results described above. Isolated LEC^{pod-low}, LEC^{pod-high}, or BECs not later than in passage 2 were grown to confluency in the lower compartments of trans-

migration chambers, and CCR10⁺ CD4⁺ CLA⁺ T lymphocytes that were purified from human peripheral blood were added to the upper chambers. Staining with anti-CLA antibody showed that these T lymphocytes were statistically significantly ($P < 0.05$) more attracted by LEC^{pod_o-low} than by LEC^{pod_o-high} or BECs. Addition of anti-CCL27 antibody with established specific inhibitory activity¹³ into the lower Transwell chamber reduced the chemoattractive capacity of LEC^{pod_o-low} to baseline levels (Figure 4D).

Discussion

As points of entrance to their journey toward the local lymph node and eventually into the venous blood stream, passenger cells access the lymphatic vasculature that is organized in blind ending, initial capillaries, precollectors, and collectors. Here, we provide evidence that specialized lymphatic endothelial cells with distinct gene expression signatures constitute initial capillaries and precollectors. Notably, the expression of pro-inflammatory chemokines is restricted to different lymphovascular segments, and we present arguments that this could be of relevance in inflammatory processes.

The major novel finding in this report is that initial lymphatic capillaries and precollectors are endowed with two distinctly different subpopulations of endothelial cells. LEC heterogeneity was initially discovered by virtue of the differential expression of the LEC-specific membrane sialomucin podoplanin, and was extended further to several other significant differences in gene expression, including characteristic gene expression of different sets of chemokines and their receptors, suggesting potentially different functions in normal tissues and in inflammatory processes. For example, LEC^{pod_o-low} in precollectors highly up-regulated CCL27, whereas CCL21 was characteristically expressed by LEC^{pod_o-high} in initial capillaries. Previous work has raised the possibility that podoplanin is involved in the generation of chemotactic gradients around initial capillaries, because CCL21 that attracts CCR7⁺ dendritic cells and T lymphocytes¹⁴ avidly bound to podoplanin and complexes were shed from the surfaces of LEC.¹⁵ Recently, experimental evidence was provided that the interaction of CCL21/CCR7 is involved in clearing sporadic CCR7⁺ cells from normal skin.¹⁶

The discovery that LEC^{pod_o-low} in lymphatic precollectors produce CCL27 raised the possibility that this vascular segment could be involved in trafficking of pathogenic CCR10⁺ T cells.¹³ These lymphocytes are the principal pathogenic effector cells in inflammatory skin diseases and in graft-versus-host reactions,¹⁷ constituting >95% of the inflammatory infiltrate. Their import route was recently mapped out in detail: CCL27 is produced by inflammatory chemokine-activated epidermal keratinocytes and diffuses toward blood microvessels.¹³ There, it is presented at the vascular lumen to attract circulating CCR10⁺ T lymphocytes and to initiate their emigration into the stroma. The indispensable role of CCL27 in this process was demonstrated by abrogation of experimental

murine dermatitis by neutralizing CCL27 antibodies.^{13,18} These results on the CCL27-driven mechanisms of lymphocyte entrance into the site of inflammation then raise the question of what the role of CCL27 secreting LEC^{pod_o-low} in lymphatic precollectors could be. We provide arguments that this segment of the lymphatic microvasculature could serve as exit route for CCR10⁺CLA⁺ T cells toward the regional lymph node. First, this view is based on a quantitative immunohistological analysis of 15 cases of human inflammatory skin disease that shows a significant selective recruitment of CCR10⁺CLA⁺ T lymphocytes around precollectors and within their lumen, in contrast to initial capillaries. Second, *in vitro* transmigration assays using cultured LEC^{pod_o-low} indicate that CCL27 secreted by these cells into the medium drives the transmigration of isolated human CCR10⁺CLA⁺ T cells. The efficiency of precollectors as potential exit gate for lymphocytes could be further enhanced by the selective presentation of endothelial adhesion proteins on LEC^{pod_o-low}, such as E-selectin, that specifically interacts with CLA on the surface of pathogenic CCR10⁺ T lymphocytes.¹⁹ Intriguingly, also cutaneous T-cell lymphoma expresses CCR10, and it remains to be determined whether any interaction with LEC^{pod_o-low} occurs and is related to their dissemination.²⁰

Expression of CCR10 was observed not only in T lymphocytes but also in LEC^{pod_o-low} in inflamed tissues (Figure 4) and was detected in cultured LECs after exposure to TNF α *in vitro*,²¹ suggesting an autocrine regulatory system that requires further elucidation. Also, the functional significance of other gene products expressed preferentially by LEC^{pod_o-low}, such as CXCL12 and CXCL14, remains to be investigated.

Synoptically, our findings establish that distinct subpopulations of LECs are defined by their expression of podoplanin and distinct patterns of chemokines. We further show that these LEC subtypes constitute different segments of the initial lymphatic vasculature. These results dovetail into the recent findings that the CD31-containing interendothelial cell junctions of initial lymphatic capillaries differ from those in precollectors.²² Finally, our results raise the possibility that the LEC^{pod_o-low}-containing precollector segment of the lymphatic vasculature is involved in the trafficking of pathogenic CCR10⁺ T lymphocytes in inflamed tissues.

Acknowledgment

We are indebted to Anton Jäger for assistance with graphics.

References

1. Ryan TJ: Structure and function of lymphatics. *J Invest Dermatol* 1989, 93:18S–24S
2. Kriehuber E, Breiteneder-Geleff S, Groeger M, Soleiman A, Schoppmann SF, Stingl G, Kerjaschki D, Maurer D: Isolation and characterization of dermal lymphatic and blood endothelial cells reveal stable and functionally specialized cell lineages. *J Exp Med* 2001, 194:797–808
3. Wick N, Saharinen P, Saharinen J, Gurnhofer E, Steiner CW, Raab I,

- Stokic D, Giovanoli P, Buchsbaum S, Burchard A, Thurner S, Alitalo K, Kerjaschki D: Transcriptomal comparison of human dermal lymphatic endothelial cells *ex vivo* and *in vitro*. *Physiol Genomics* 2007, 28:179–192
4. Wick N, Bruck J, Gurnhofer E, Steiner CW, Giovanoli P, Kerjaschki D, Thurner S: Nonuniform hybridization: a potential source of error in oligonucleotide-chip experiments with low amounts of starting material. *Diagn Mol Pathol* 2004, 13:151–159
 5. Segerer S, Cui Y, Eitner F, Goodpaster T, Hudkins KL, Mack M, Cartron JP, Colin Y, Schlondorff D, Alpers CE: Expression of chemokines and chemokine receptors during human renal transplant rejection. *Am J Kidney Dis* 2001, 37:518–531
 6. Wasniowska K, Petit-LeRoux Y, Tournamille C, Le van Kim C, Cartron JP, Colin Y, Lisowska E, Blanchard D: Structural characterization of the epitope recognized by the new anti-Fy6 monoclonal antibody NaM 185–2C3. *Transfus Med* 2002, 12:205–211
 7. Morikawa S, Baluk P, Kaidoh T, Haskell A, Jain RK, McDonald DM: Abnormalities in pericytes on blood vessels and endothelial sprouts in tumors. *Am J Pathol* 2002, 160:985–1000
 8. Kerjaschki D, Huttary N, Raab I, Regele H, Bojarski-Nagy K, Bartel G, Krober SM, Greinix H, Rosenmaier A, Karhofer F, Wick N, Mazal PR: Lymphatic endothelial progenitor cells contribute to *de novo* lymphangiogenesis in human renal transplants. *Nat Med* 2006, 12:230–234
 9. Reiss Y, Proudfoot AE, Power CA, Campbell JJ, Butcher EC: CC chemokine receptor (CCR)4 and the CCR10 ligand cutaneous T cell-attracting chemokine (CTACK) in lymphocyte trafficking to inflamed skin. *J Exp Med* 2001, 194:1541–1547
 10. Morales J, Homey B, Vicari AP, Hudak S, Oldham E, Hedrick J, Orozco R, Copeland NG, Jenkins NA, McEvoy LM, Zlotnik A: CTACK, a skin-associated chemokine that preferentially attracts skin-homing memory T cells. *Proc Natl Acad Sci USA* 1999, 96:14470–14475
 11. Neote K, Mak JY, Kolakowski Jr LF, Schall TJ: Functional and biochemical analysis of the cloned Duffy antigen: identity with the red blood cell chemokine receptor. *Blood* 1994, 84:44–52
 12. Nagira M, Imai T, Hieshima K, Kusuda J, Ridanpaa M, Takagi S, Nishimura M, Kakizaki M, Nomiya H, Yoshie O: Molecular cloning of a novel human CC chemokine secondary lymphoid-tissue chemokine that is a potent chemoattractant for lymphocytes and mapped to chromosome 9p13. *J Biol Chem* 1997, 272:19518–19524
 13. Homey B, Alenius H, Muller A, Soto H, Bowman EP, Yuan W, McEvoy L, Lauerma AI, Assmann T, Bunemann E, Lehto M, Wolff H, Yen D, Marxhausen H, To W, Sedgwick J, Ruzicka T, Lehmann P, Zlotnik A: CCL27–CCR10 interactions regulate T cell-mediated skin inflammation. *Nat Med* 2002, 8:157–165
 14. Luther SA, Bidgol A, Hargreaves DC, Schmidt A, Xu Y, Paniyadi J, Matloubian M, Cyster JG: Differing activities of homeostatic chemokines CCL19, CCL21, and CXCL12 in lymphocyte and dendritic cell recruitment and lymphoid neogenesis. *J Immunol* 2002, 169:424–433
 15. Kerjaschki D, Regele HM, Moosberger I, Nagy-Bojarski K, Watschinger B, Soleiman A, Birner P, Krieger S, Hovorka A, Silberhumer G, Laakkonen P, Petrova T, Langer B, Raab I: Lymphatic neoangiogenesis in human kidney transplants is associated with immunologically active lymphocytic infiltrates. *J Am Soc Nephrol* 2004, 15:603–612
 16. Debes GF, Arnold CN, Young AJ, Krautwald S, Lipp M, Hay JB, Butcher EC: Chemokine receptor CCR7 required for T lymphocyte exit from peripheral tissues. *Nat Immunol* 2005, 6:889–894
 17. Faaij CM, Lankester AC, Spierings E, Hoogeboom M, Bowman EP, Bierings M, Revesz T, Egele RM, van Tol MJ, Annels NE: A possible role for CCL27/CTACK–CCR10 interaction in recruiting CD4 T cells to skin in human graft-versus-host disease. *Br J Haematol* 2006, 133:538–549
 18. Chen L, Lin SX, Agha-Majzoub R, Overbergh L, Mathieu C, Chan LS: CCL27 is a critical factor for the development of atopic dermatitis in the keratin-14 IL-4 transgenic mouse model. *Int Immunol* 2006, 18:1233–1242
 19. Berg EL, Yoshino T, Rott LS, Robinson MK, Warnock RA, Kishimoto TK, Picker LJ, Butcher EC: The cutaneous lymphocyte antigen is a skin lymphocyte homing receptor for the vascular lectin endothelial cell-leukocyte adhesion molecule 1. *J Exp Med* 1991, 174:1461–1466
 20. Notohamiprodjo M, Segerer S, Huss R, Hildebrandt B, Soler D, Djafarzadeh R, Buck W, Nelson PJ, von Luettichau I: CCR10 is expressed in cutaneous T-cell lymphoma. *Int J Cancer* 2005, 115:641–647
 21. Johnson LA, Clasper S, Holt AP, Lalor PF, Baban D, Jackson DG: An inflammation-induced mechanism for leukocyte transmigration across lymphatic vessel endothelium. *J Exp Med* 2006, 203:2763–2777
 22. Baluk P, Fuxe J, Hashizume H, Romano T, Lashnits E, Butz S, Vestweber D, Corada M, Molendini C, Dejana E, McDonald DM: Functionally specialized junctions between endothelial cells of lymphatic vessels. *J Exp Med*. 2007, 204:2349–2362